



LAWRENCE  
LIVERMORE  
NATIONAL  
LABORATORY

# INFLUENCE OF POROSITY ON IMPULSIVE ASTEROID MITIGATION SCENARIOS

E. B. Herbold, D. Dearborn, P. Miller

April 8, 2015

2015 IAA Planetary Defense Conference  
Frascati, Italy  
April 13, 2015 through April 17, 2015

## **Disclaimer**

---

This document was prepared as an account of work sponsored by an agency of the United States government. Neither the United States government nor Lawrence Livermore National Security, LLC, nor any of their employees makes any warranty, expressed or implied, or assumes any legal liability or responsibility for the accuracy, completeness, or usefulness of any information, apparatus, product, or process disclosed, or represents that its use would not infringe privately owned rights. Reference herein to any specific commercial product, process, or service by trade name, trademark, manufacturer, or otherwise does not necessarily constitute or imply its endorsement, recommendation, or favoring by the United States government or Lawrence Livermore National Security, LLC. The views and opinions of authors expressed herein do not necessarily state or reflect those of the United States government or Lawrence Livermore National Security, LLC, and shall not be used for advertising or product endorsement purposes.

IAA-PDC-15-03-03  
 INFLUENCE OF POROSITY ON IMPULSIVE ASTEROID MITIGATION SCENARIOS

Eric B. Herbold<sup>(1)</sup>, David Dearborn, Paul Miller

<sup>(1)</sup>Lawrence Livermore National Laboratory, P.O. Box 808, Livermore, CA, 94551; (925)422-1659, herbold1@llnl.gov

**Keywords:** porosity, deflection, disruption, numerical modeling

**INTRODUCTION**

The morphological and mechanical properties of asteroids play a significant role in determining the response to impulsive-deflection strategies for potentially hazardous objects on paths towards Earth. The wide variation in composition, material state and structure of asteroids constitute a significant barrier to understand their response to impulsive loading. The role of porosity and strength of fractured and gravitationally consolidated “rubble pile” asteroids to a standoff explosion or high-velocity impact are investigated here for nominally spherical objects considered for the 2015 PDC hypothetical asteroid-impact scenario [1]. The interplay between micro- and macro-scale porosity and material strength are compared between these two different scenarios. Scaling laws between strength and porosity are known for several terrestrial rock types (e.g. sandstone, limestone) and are considered here in the absence of detailed knowledge of an asteroid’s material composition. Energy deposition profiles are considered here in one and three dimensions measuring the melt depth as a function of initial porosity and disruption velocity distributions for different materials.

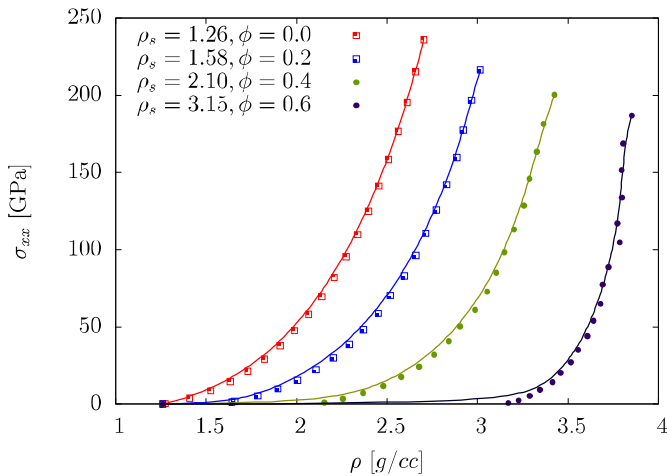


**Figure 1: 1-dimensional shock loading results from 0.1-20 km/s for 4 different simulated materials (based on chondrite equation of state data) with the same initial density.**

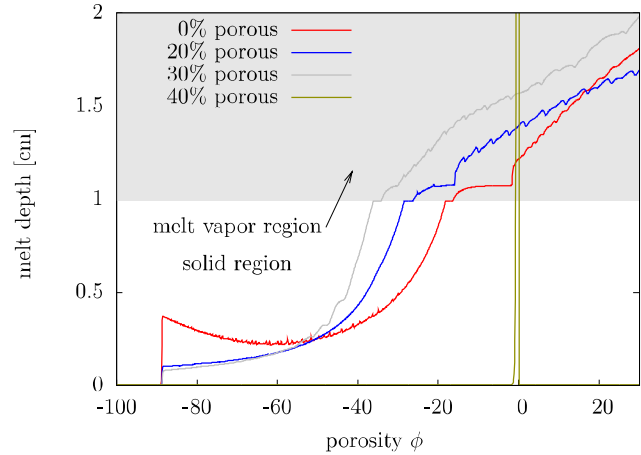


**Figure 2: Comparison of melt depths for four different materials with an energy deposition of  $1.4 \cdot 10^4$  J/mm<sup>2</sup>. The initial deposition profile produces a dispersive pulse in all cases up to 40% porosity, where the pore space is not closed enough to produce an acoustic pulse.**

**ENERGY DEPOSITION AND MELT DEPTH**

Impulsive loading of loosely consolidated “rubble pile” asteroids has been considered in [2], with the individual boulders treated as rigid bodies. Recently, [3] investigated the effects of micro- and macroporosity on the  $\beta$  factor in simulations of asteroid impacts. It is likely that the density of a potentially threatening object will be known more accurately than its composition. This means that deflection or disruption scenarios will be constrained by knowing the mass and speed of the object, but very little about the possible mechanical response. The authors in [4] suggest that the majority of near earth objects (NEO) may be categorized within the LL chondrites, which is a small fraction of the vast material types present within the overall asteroid population. The porosity may vary widely within the NEO population [5,6], which means the compressibility of the asteroid bulk material may vary widely as shown in Figure 1, where four different materials have been constructed based on a Tillotson equation of state fit to shock loading data for hydrated chondrites. The initial density of each material shown is 1.26 g/cc, which is the reported value for 101955 Bennu from [7]. For each

material, the solid equation of state parameters were unchanged except for the solid density such that  $\rho_0 = \rho_s(1 - \phi_0) = 1.26$ . The solid density values are also listed in **Figure 1**. Note that the highly porous material is less stiff for lower pressures, but for higher pressures compaction and bulking processes heat the material more than a nonporous material.

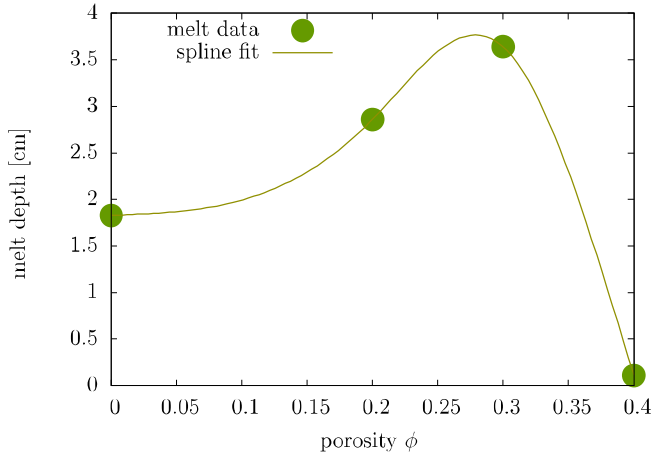


**Figure 3: Melt depth measurements for the four materials shown in Figure 2.**

In Figure 2 a comparison of melt depths for four different materials with an energy deposition of  $1.4 \cdot 10^4$  J/mm<sup>2</sup> described in Managan, et. al. (IAA-PDC-15-P-53). The initial deposition profile produces a dispersive pulse in all cases up to 40% porosity, where the pore space is not closed enough to produce an appreciable acoustic pulse. The energy deposition profile melts to depths depending on the initial porosity. It should be emphasized that the spline fit shown in Figure 3 is only included to indicate that very high levels of porosity may not produce an acoustic pulse, which may affect the melt depth by an order of magnitude. It is interesting that the melt depth due to the passage of a shock-like pulse increases with porosity. This may be due to the additional heating due to porous compaction, but a more systematic investigation is needed to be sure.

### DEFLECTION SCENARIOS

The response of different asteroid structures largely depends on where the porosity resides. In **Figure 4**, a sectioned view of a “rubble pile” and fractured consolidated asteroid are subjected to the same standoff explosion where 5 kt was coupled to the outermost layer of the finite element mesh using a LLNL parallel Lagrangian finite element code named GEODYN-L, which is capable of large deformation, contact, fracture, erosion and particle conversion. **Figure 4** elucidates the large difference in wave propagation depending on the internal structure. The “rubble pile” asteroid transmits information through the material via contacting boulders with small contact patches, while the fractured

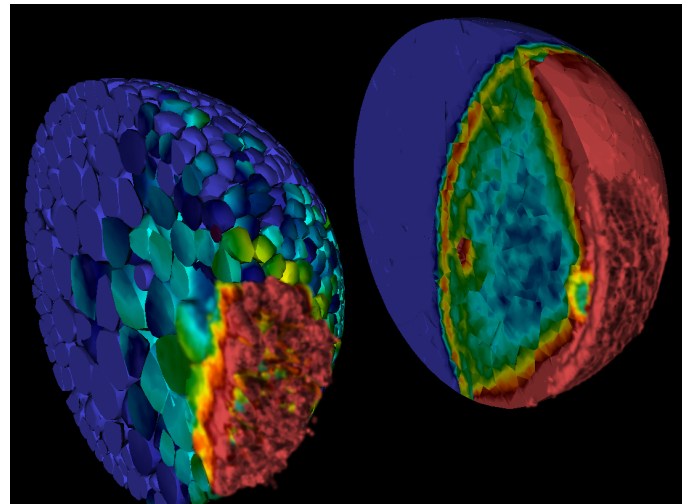


**Figure 4: Sectioned view of standoff-explosion results comparing the response of a nominally 500-m-diameter gravitational aggregate (left) and fractured consolidated body (right) at times  $t = 0.9$  s and  $t = 7.1$  s respectively. The color variation shows the velocity magnitude ranging from 0 - 1 m/s.**

consolidated body is much more efficient at propagating waves. There is almost an order of magnitude difference in time when the impulse has propagated halfway across the simulated asteroid (0.9 s compared to 7.1 s). It is also clear that the impulse is influenced by the internal structure of the asteroid that can affect the dispersion velocity of the individual pieces once the initial impulse has passed through the entire body. Tracking the statistical motion of resultant pieces is important for deflection or disruption assessments, and are shown in Figure 5 and Figure 6.

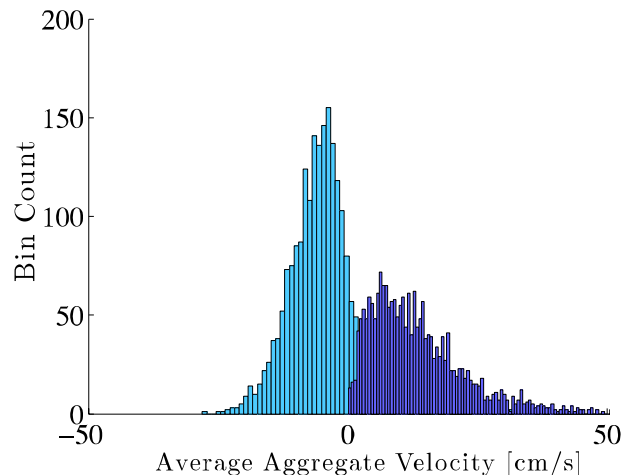


**Figure 5: Velocity distribution of 2380 boulders from a GEODYN-L simulation where 5.4 kt was deposited into a regolith layer. The material in this calculation had a porosity of 8.6% and macroporosity of 21.4% for 30% total porosity.**

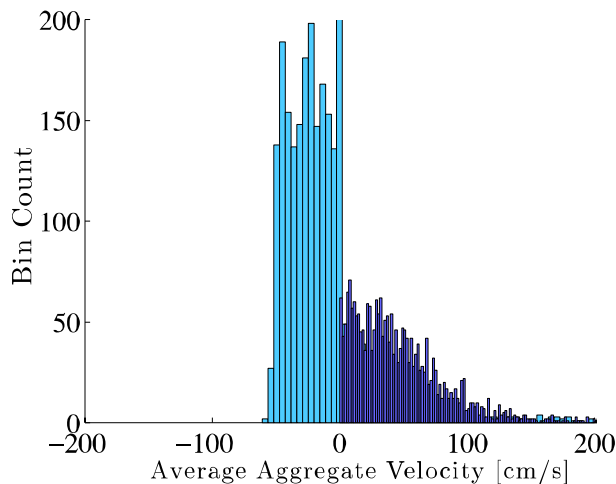


**Figure 6: Velocity distribution of 2380 boulders from a GEODYN-L simulation where 5.4 kt was deposited into a regolith layer. The material in this calculation has a 30% microporosity and the boulders were meshed separately such that they do not support tension.**

In Figure 5 the velocity distribution for 2380 boulders is shown for the radial and axial direction for the rubble-pile object shown on the left side of Figure 4. The resultant deflection velocity distribution has a mean of approximately 5 cm/s and a mass weighted average of 7.8 cm/s. The shape of the velocity distribution is described well by a normal PDF. In contrast, the mean value of the axial deflection velocity shown in Figure 6 is much larger (approximately 12.5 cm/s), but the mass weighted average of the boulder deflection velocity is lower at 6.9 cm/s. The overall initial object mass and deposited energy were identical for both scenarios.

The 13% increase in deflection velocity for the rubble-pile asteroid may be attributed to the ~8 time difference in pulse propagation across each body as shown in Figure 4 noting that the ejecta above escape velocity changes in time such that the deflection momentum converges to a final value. In other words, some error is expected for the deflection velocity measurement due to this time dependent process. Differences may also arise due to the contact surface between the meshed regolith layer (not shown) and the underlying boulders. However, from Figure 3 it was observed that higher porosity material (around 30%) produced a greater melt depth than lower porosity material.

Both simulated objects have an overall porosity of 30% and, in the case of the rubble-pile asteroid, the individual boulders have a porosity of 8.6%. It may be reasonable to assume that the melt depth would be lower for the 8.6% porous material compared with the 30% porous material in the fractured consolidated body, which contrasts the mass averaged deflection velocity results.

Further investigation is required to better assess these differences.

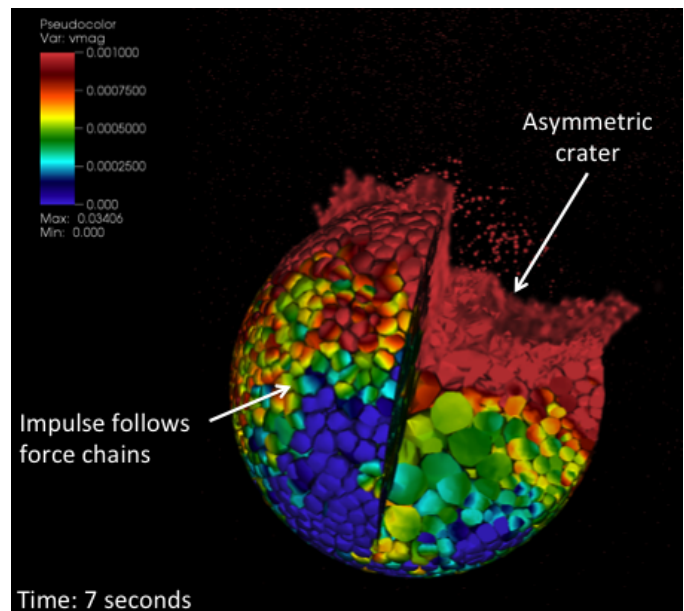


**Figure 7: GEODYN-L simulation of a rubble-pile object with 50 kt energy deposited into a regolith cap. Much more material is excavated than in Figure 4. It is also observed that the heterogeneity in the packing structure of the boulders produces an asymmetric crater. It should be emphasized that surface effects such as the trajectory of the blowoff causing angular momentum changes should also extend to the object's interior, since the internal structure may belie a smooth outer surface.**

In Figure 7 the rubble pile object is subjected to a 50 kt deposition layer and shown at 7 s similar to Figure 4. The velocity magnitude distribution (in mm/ $\mu$ s) has a range only for densities >1.9 g/cc (i.e. lower density material is traveling much faster). Also included in this figure are discrete particles away from the crater shape which are formed when finite elements attain a density lower than 0.1 g/cc or a plastic strain >3.0. An asymmetric crater is clearly visible. It is interesting to note that a nominally spherical object may eject material asymmetrically due to the underlying heterogeneity. This is an important observation as it is a more subtle point than accounting for surface topology alone.

## CONCLUSIONS

For impacts and standoff explosions alike, high porosity (micro, macro or combined) may prohibit shock wave generation. Comparing 4 materials with different porosities ranging from 0-60%, a shock was not produced for porosities above 40%. This affects the melt depth by over an order of magnitude in 1d simulations. The internal structure of asteroid objects affects the dispersion of fragments meaning that if external symmetry is observed it does not necessarily

indicate that one should expect a symmetric response. This also means that standoff explosions and normal impacts alike may produce rotation in the remaining object (i.e. with velocity lower than the escape value) simply due to the internal structure of the asteroid.

## ACKNOWLEDGEMENTS

Part of this work was funded by the Laboratory Directed Research and Development Program at LLNL under project tracking code 12-ERD-005, performed under the auspices of the U.S. Department of Energy by Lawrence Livermore National Laboratory under Contract DE-AC52-07NA27344. LLNL-ABS-669475.

## REFERENCES

- [1] <http://neo.jpl.nasa.gov/pdc15/>. The 2015 PDC Hypothetical Asteroid Impact Scenario.
- [2] Korycansky DG, Plesko CS. *Acta Astronaut* 2012;73:10.
- [3] Jutzi M, Michel P. *Icarus* 2014;229:247.
- [4] Vernazza P, Binzel RP, Thomas C a, DeMeo FE, Bus SJ, Rivkin a S, Tokunaga a T. *Nature* 2008;454:858.
- [5] Consolmagno GJ, Britt DT, Macke RJ. *Chemie der Erde - Geochemistry* 2008;68:1.
- [6] Britt DT, Yeomans D, Housen K, Consolmagno G. Asteroid Density, Porosity, and Structure, in: Bottke Jr. WF, Cellino A, Paolicchi P, Binzel RP (Eds.). *Asteroids III*. Tucson: University of Arizona Press, Tucson; 1999.
- [7] Chesley SR, Farnocchia D, Nolan MC, Vokrouhlický D, Chodas PW, Milani A, Spoto F, Rozitis B, Benner L a. M, Bottke WF, Busch MW, Emery JP, Howell ES, Lauretta DS, Margot J-L, Taylor P a. *Icarus* 2014;235:5.